Characterization of electroplated Ni/SiC and Ni/Al_2O_3 composite coatings bearing nanoparticles

Sheng-Chang Wang and Wen-Cheng J. Wei[a)]
Institute of Materials Science and Engineering, National Taiwan University, Taipei, Taiwan 106, Republic of China

(Received 10 November 2002; accepted 9 April 2003)

Ultrafine SiC and Al_2O_3 particles with 30–50 nm sizes were used to codeposit with Ni in a sulfamate bath to form composite coatings. The microstructure and mechanical properties of the layers were investigated by x-ray diffractometry, scanning and transmission electron microscopy, high-resolution transmission electron microscopy, microindentation, and wear testing. The microstructural results revealed that 7 vol% of SiC or Al_2O_3 particles dispersed randomly in the Ni matrix. The addition of the ultrafine SiC or Al_2O_3 powder into the Ni matrix apparently reduced the size of Ni grains during the electroplating and inhibited the grain growth during heat treatment. The microhardness and wear resistance were improved by the addition of SiC and Al_2O_3 particles, especially for SiC/Ni samples after heat treatment at 400 °C for 24 h. The mechanisms of hardening and wearing of Ni-based electroplated layers are discussed.

I. INTRODUCTION

Composite coatings or electrolytic codepositions are prepared by dispersing insoluble ceramic, polymeric, or metallic powders in an electroplating solution during metal electroplating. The simultaneous deposition of the particulate inclusions and metal phase to form composite coating results in an improvement of physical and mechanical properties. Recently, a technical breakthrough was appreciated on the application of the codeposited composite with the hardened layers on the cylinder surface of a hot engine,[1] or the surface of a cooling Cu mold for continuous casting of molten steel.

The ceramic particles reported in the literature could be Al_2O_3, ZrO_2, SiC, diamond, Cr_2O_3, TiO_2, MoS_2, and WC.[2–14] Among these inclusions, SiC is one of the important ceramic materials for structural and electronic applications. SiC has high resistance to wear because of its large hardness, thermal shock, chemical corrosion resistance, and good stability at high temperature, which is mainly due to its covalent bonding character. Therefore, SiC has been widely used as an abrasive and the materials for hot ceramic engine and heating elements.[15,16]

Hard particles, in general, improve the hardness and tribological properties of the composite Ni layer by the dispersively strengthening mechanism. The hard inclusions can inhibit the movement of grain boundaries of Ni grains and retard the grain growth during thermal treatment. When the material suffers an external stress, the inclusions hinder the dislocation movement in metallic matrix, whereby plastic deformation becomes difficult.[17] Therefore, the hardness of the composite layer increases, and the wear resistance can be improved. Besides, the wear resistance can also be improved by reducing the grain size of the metal matrix, which includes ceramic particles at grain boundaries.[18]

According to Orowan's report, the mechanism for dispersive hardening occurs in composite systems, the lowest stress (τ_0) required to force the dislocation between the particles is[17]

$$\tau_0 \approx \frac{Gb}{\lambda} \quad , \tag{1}$$

where G is the shear modulus, b is the Burgers vector of the dislocation tied with two particles, and λ is the distance between two particles. When the number of hard inclusions increases and is well dispersed in the matrix, the average particle distance λ reduces, and a hardening composite coating can be prepared. Therefore, the strengthening effects can be enhanced by using nanoparticles in electroplating composites.

In this study, ultrafine SiC and Al_2O_3 particles were used as dispersoids to improve the tribological properties of the SiC/Ni composite layer, which was prepared by composite plating. We attempted to find out the influence

a)Address all correspondence to this author.
1 Roosevelt Road, Sec. 4, Taipei, Taiwan 106, Republic of China.
e-mail: wjwei@ccms.ntu.edu.tw

of different types of ceramic particles and the particle size of the secondary phase in the composites. The change of microstructure, of course, is controlled by the presence of fine SiC and Al_2O_3, and may result in a great improvement on the mechanical properties (e.g., hardness and wear resistance), especially at an elevated temperature.

II. EXPERIMENTAL

Two kinds of nano-sized ceramic powders were used in this study; one is a plasma-synthesized SiC (PJ-PL-SiC, PlasmaChem, GmbH, Germany), and the other is a spherical Al_2O_3 powder (PJ-PL-ALO, Wah Lee, Taipei, Taiwan). The ultrafine SiC powder shows a major phase 3C, and the average particle size is 62 nm. The Al_2O_3 powder has an average particle size of 30 nm with the δ phase.

For the composite plating, a nickel sulfamate bath containing 90 g/l nickel sulfamate (EP grade, Phibrochem Inc., Fort Lee, NJ), 3 g/l nickel chloride (EP grade, SHOWA, Gyoda City, Saitama, Japan), and 40 g/l boric acid (EP grade, SHOWA, Japan) were used. A copper plate with dimensions of $10 \times 6.5 \times 0.25$ mm^3 was used as cathode, and the anode was a Ti basket containing small nickel ingots. Before plating, a sequence of cleaning and acidic etching of the Cu plate by diluted sulfuric acid was carried out to remove the contamination and greasiness on the surface.

The solid loading of the suspended powder in the plating solution was 1 vol% (32 g/l for SiC and 39 g/l for Al_2O_3) based on the bath volume. Gentle stirring of the suspension by air bubbles kept the solution well dispersed. The current density applied for the electroplating was 4 A/dm^2 ampere per square decimeter (ASD). The bath temperature was controlled at 50 ± 2 °C, and the pH ranged from 4.0 to 5.0, which was adjusted by H_3BO_3 or $NiCO_3$. In this study, three types of pure Ni layer were prepared by pulse-plating to reduce Ni grain size. A periodical square wave was used with the condition of current density of 8 ASD (peak current density), and the on and off times were 3 and 1 ms, respectively.

Crystalline phases of the coated layers were identified by x-ray diffractometry (XRD; PW1792, Philips Instrument, Eindhoven, The Netherlands). A cross section of the codeposition layer was cut and polished and examined with scanning electron microscopy (SEM; XL30 Philips, Netherlands) equipped with an energy-dispersive spectrometer (EDS; DX4, EDAX Corporation, Mahwah, NJ). Thin foil specimens for transmission electron microscopy (TEM) observation were prepared by several steps. The cross section of the composite layer was cut to a thin disk; then the disk was ground and polished to reduce its thickness to 30 μm or less. After that, a thin section was glued on a copper ring 3 mm in diameter and milled by Ar ions (Precision ion-polishing system, M-691, Gatan, Warrendale, PA) until a thinned region was observed to the area of interest. The microstructures were characterized by TEM (100CXII), high-resolution TEM (HRTEM; FX-400E, JEOL, Tokyo, Japan) or high-resolution analytical electron microscopy (HRAEM; Hitachi HF-2000, Tokyo, Japan) equipped with energy dispersive x-ray (EDX; Noran, Voyager1000, Boston, MA).

In this study, the fraction of second phase in the composites was measured by quantitative image analysis technique. The SEM images were taken and processed by the backscattered imaging mode. The images of SiC and Al_2O_3 particles appear in darker contrast than the Ni matrix. The volume fraction of the second phase can be calculated by integrating the darker features over the total area of the image.

To understand the degradation of the hardness at high temperatures, the coating samples were heat treated in an atmosphere-controlled furnace vented with N_2 and operated at 400 °C for 24 h, or kept at constant temperatures either at 100, 200 °C, . . . or 600 °C for 1 h. The hardness of the cross section of the layer was measured by a Vicker's indentor (AKASHI, MVK-EII, Tokyo, Japan) with a load of 100 gf and lasted for 15 s. The tribological properties of the composite layer, including wear resistance and friction coefficient, were measured by a block-on-wheel method (TE53, Plint & Partiners Ltd., Newbury, United Kingdom). The wearing wheel was made by a heat-treated steel (NSOH/B01) (Plint & Partiners Ltd.) with a hardness 65 HRc (830 HV). The block specimens in a cross section of 5×13 mm^2 were tested with a load of 67 N and in air of 65% relative humidity at 22 °C. The rotational speed of the wheel was 200 rpm, and the numbers of cycles were between 3000 and 8000.

III. RESULTS

Figure 1 shows the XRD results of pure Ni, SiC/Ni, and Al_2O_3/Ni composite layers prepared by electroplating. Because the diffraction intensity of the ultrafine ceramic particles is very weak relative to the metal Ni, only rescaled spectra of the strongest peaks of SiC $(10\bar{1}2)_{6H}$ and Al_2O_3 $(4\ 4\ 0)_{\delta}$ are visible in the insets of Fig. 1. According to the JCPDS file of Ni,[19] the relative intensity ratio of the three strongest planes (111), (200), and (220) are 100:42:21. Compared with the same Ni planes in this study, the ratio of pure Ni shown in Fig. 1 is 40:8:100, and the ratio of ultrafine SiC/Ni or Al_2O_3/Ni is close to 100:10:4. Obviously, the preferred plane of the pure Ni prepared by the electroplating process is $(220)_{Ni}$. When the ultrafine SiC or Al_2O_3 particles are added into the Ni matrix, the preferred orientation changes to $(111)_{Ni}$ plane.

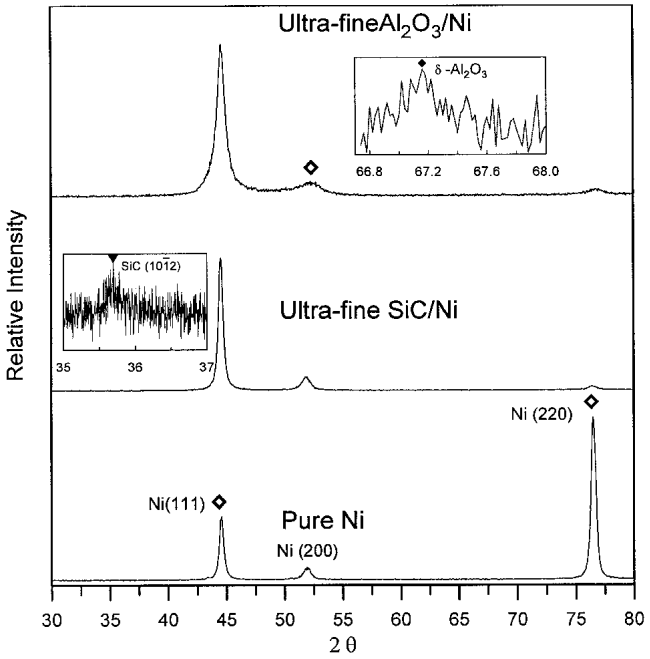

FIG. 1. XRD patterns of pure Ni and ultrafine SiC/Ni and Al_2O_3/Ni composite layers.

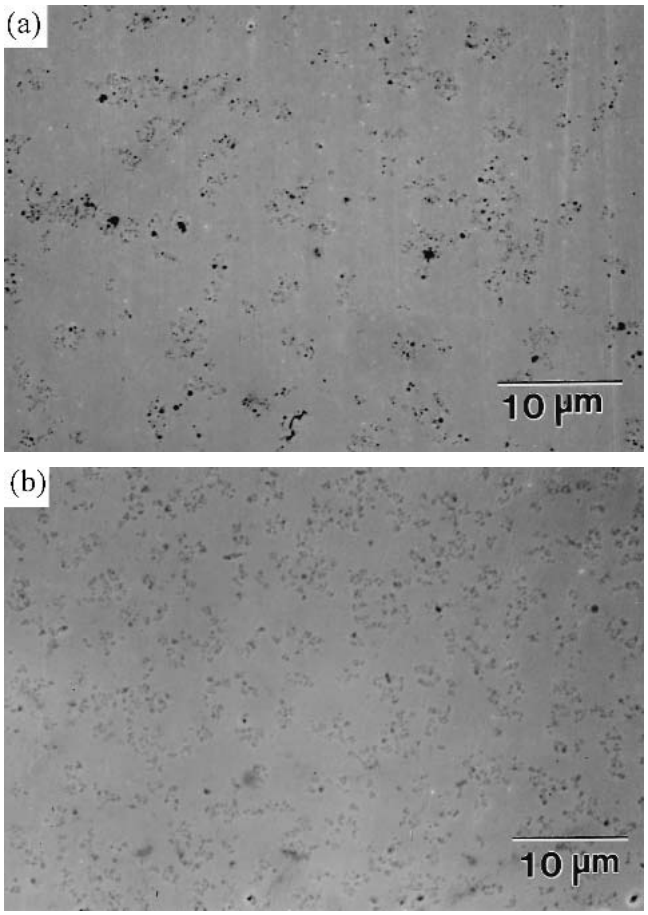

FIG. 2. SEM micrographs of (a) ultrafine SiC/Ni, and (b) ultrafine Al_2O_3/Ni composites.

The cross sections of the SEM micrographs, as shown in Fig. 2, display the distribution of ultrafine SiC and ultrafine Al_2O_3 in the Ni matrix. The ceramic particle content for both composite layers is 7 vol%, which is an optimal content prepared under the present electroplating conditions.[20] The SiC particles show a random distribution in the Ni matrix, and individual clustering features appear 0.1 μm in size, which can be found in the highly magnified images. The individual size is close to the mean particle size of SiC detected by TEM. This indicates that the SiC particles in the electroplating solution are well dispersed, and the agglomeration of SiC in the electroplating solution hardly occurs.

Figure 3 shows the TEM micrographs of the cross section of pure Ni, ultrafine SiC/Ni, and ultrafine Al_2O_3/Ni composite layers. The Ni grains in the pure Ni specimen without any powder show columnar grains with the longitudinal axis and growth direction perpendicular to the Cu substrate. The average grain dimensions are 0.23 μm in diameter and 2–3 μm in length. However, for an as-plated composite specimen with ultrafine SiC or Al_2O_3 particles, the mean grain size of the Ni reduces to 78 and 89 nm, respectively, and the shape becomes equiaxial due to the presence of the second phases.

In the HRTEM observation with EDS analysis, an amorphous SiO_2 layer appears on the surface of SiC particles. Two types of the interfaces between SiC and Ni can be distinguished from the observation of the microstructures. One appears voids and cracks at the interface [Fig. 4(a)]. The surface of the SiC particle shows a SiO_2 layer with a thickness greater than 5–10 nm. The other type has an intact interface [Fig. 4(b)], which shows a thin and uniform SiO_2 layer about 5 nm thick [Fig. 4(c)].

Figure 5 shows the lattice image of two partially adhered Al_2O_3 particles embedded in Ni matrix. An amorphous layer was found on the surface of the Al_2O_3 particle. The interface between Al_2O_3 and Ni is integrated. As marked in Fig. 5, the Ni grains located at the concave region of the adhesive Al_2O_3 particles show several Moiré fringes, which indicate the interference between two Ni grains having similar orientation, but rotating each other at a small angle. The tiny Ni grains may grow and gradually fill the concave space. This implies that the concave surface of ceramic phases can be the heterogeneous nucleation sizes of Ni grain during the electroplating. Thus, the final size of Ni grains in the composite is limited due to a higher nucleation density. As can be concluded from Figs. 3 and 5, the microstructure evidence shows that addition of the nano-sized SiC and Al_2O_3 particles into the Ni matrix apparently refine the grain size of the Ni matrix and change the grain shape from columnar to equiaxial.

Figure 6 shows the evolution of the friction coefficient (μ) of the SiC/Ni and Al_2O_3/Ni composites compared

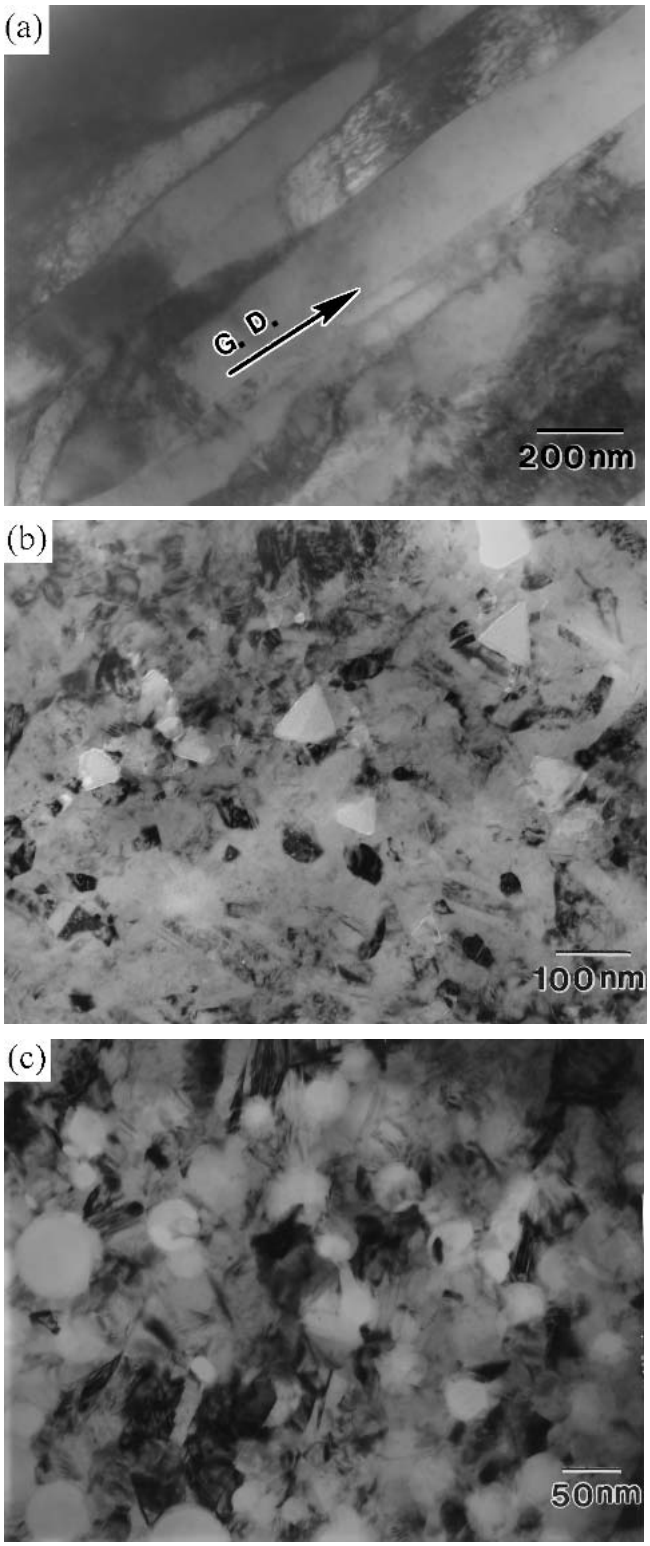

FIG. 3. TEM micrographs of the cross section of (a) pure Ni and ultrafine (b) SiC/Ni and (c) Al_2O_3/Ni composite layers.

to that of a pure Ni coating. The friction coefficient is independent of the wear time and seems to remain in the same level after heat treatment at 400 °C. Although the values of the friction coefficient are fairly close between these three kinds of deposited layers, pure Ni seems to have the smallest value. The higher friction coefficient of SiC/Ni and Al_2O_3/Ni composites may be partially due to the fact that the presence of nano-sized SiC and Al_2O_3 particles induced greater lateral forces, which are due to the interaction of the particles to the wearing wheel during sliding.

The wear results for the composite layers and pure Ni are plotted in Fig. 7. The wear rate of the SiC/Ni or Al_2O_3/Ni composite layer without heat treatment is an average of 6×10^{-9} or 8×10^{-9} cm^3/N m, respectively. It is better than that of pure Ni. Moreover, after 400 °C heat treatment for 24 h, the wear rate of the treated composite layers remains at a similar level, while the wear rate of the treated pure Ni increases about 50 times.

Figure 8 shows that the hardness of ultrafine SiC/Ni and Al_2O_3/Ni composite layers and the hardness and grain size of pure Ni changed with annealing temperatures. At room temperature, the hardness of the composite layer is greater than that of the pure Ni layer. When the specimens were treated at specified temperatures for 1 h, the hardness of three Ni coatings dramatically decreased at about 300 °C. The SiC/Ni composite layer has the highest hardness at all testing temperatures among these Ni coated layers. When the heat-treatment temperature is higher than 300 °C, the hardness of the composite layers decreases to 250–300 HV. The grains of pure Ni grew to larger sizes at higher heat-treatment temperatures for 1 h (Fig. 8). This causes the softening of Ni matrix.

IV. DISCUSSION

A. Hardening effects by ultrafine particulates

There are two possible hardening mechanisms for the Ni composite layers incorporated with nanoparticulates. One is the refinement of the grain size, which can be described simply by a Hall–Petch (H-P) effect.[21] The other is from the contribution of hard particles, which show a dispersive hardening effect (Orowan dislocation bowing model). SEM micrographs of the acid-etched surfaces of the pure Ni and the SiC/Ni and Al_2O_3/Ni composites are shown in Fig. 9. All three specimens were heat treated at 400 °C for 24 h. The Ni grains grew to micrometric sizes. The average Ni grain size of the treated pure Ni, SiC/Ni, and Al_2O_3/Ni are 14, 1.0, and 1.4 μm, respectively. The data depict that the growth of Ni is significantly retarded by the SiC and Al_2O_3 particulates at 400 °C (compared with the pure Ni sample).

The microstructural and mechanical properties of the pure Ni layer and composite layers in this study are summarized in Table I. The average Ni grain size of the composite layers is strongly related to the hardness properties. When the hardness and the grain size (d) of the Ni

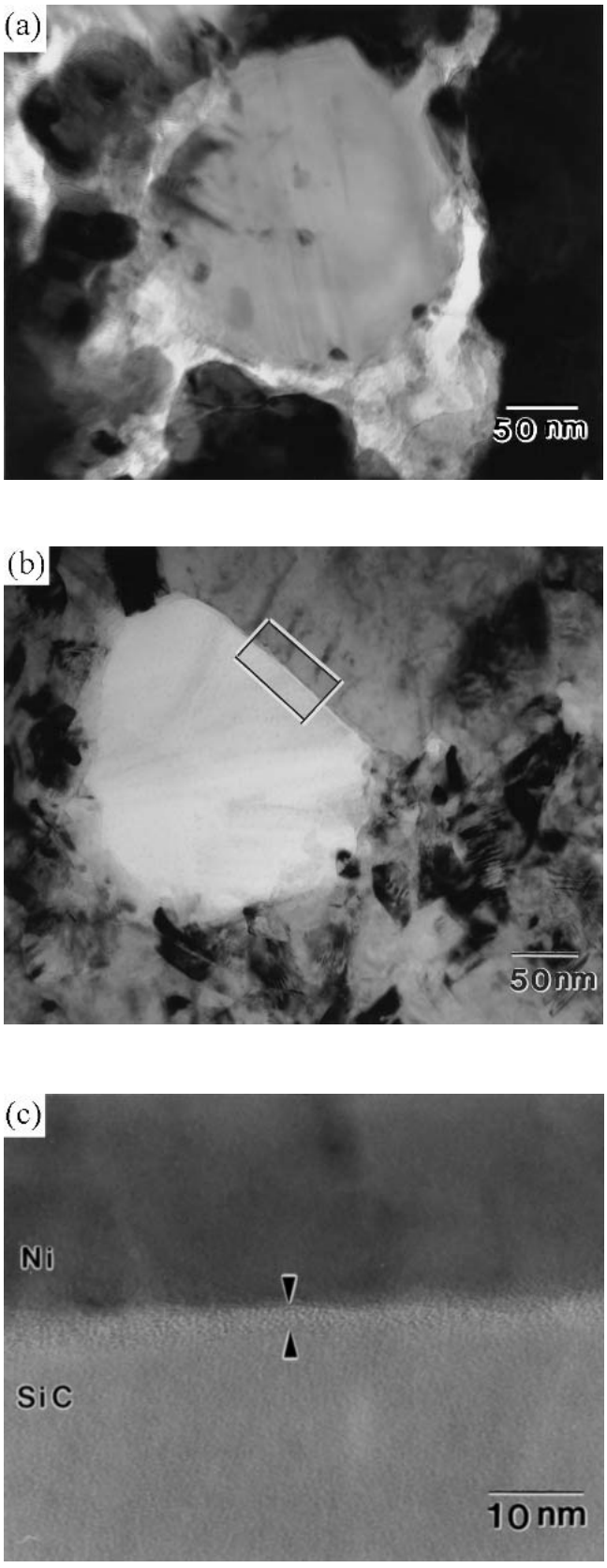

FIG. 4. HRTEM micrographs revealing the interfaces of SiC and Ni: (a) particle with thick SiO_2 scale, (b) with a thin silica layer, and (c) lattice image of the interface in (b).

grain in the three kinds layers are formularized by the Hall–Petch relationship, the data can be plotted, as shown in Fig. 10. It shows that the hardness increases with the refinement of Ni grain. El-Sherik *et al.* showed that the hardness of the pure Ni prepared by electroplating followed regular Hall–Petch behavior for the grain size larger than 100 nm.[22] When the Ni grain size was smaller than the 20 nm, a plateau in the hardness curve was observed. Their data are also shown in Fig. 10. The deviation from the Hall–Petch behavior was suggested due to a softening mechanism associated with abundant

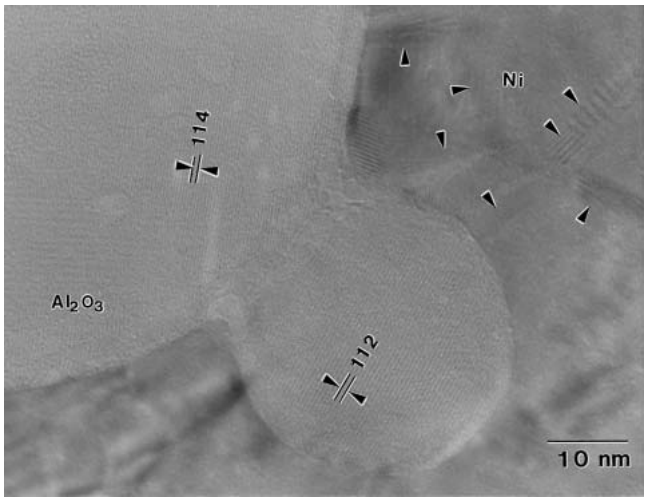

FIG. 5. HRTEM micrograph of the lattice image of the interface of Al_2O_3 and Ni.

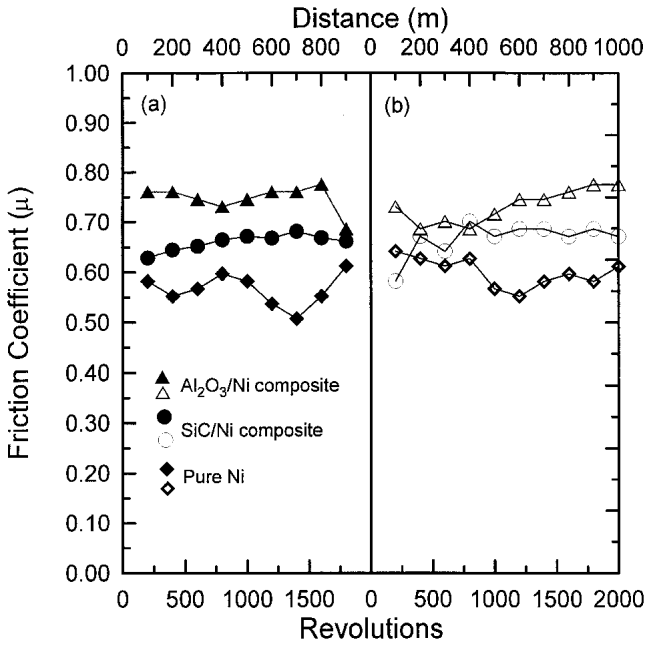

FIG. 6. The friction coefficient of the pure Ni and ultrafine SiC/Ni and Al_2O_3/Ni composite layers worn against tempered steel: (a) as-plated and (b) heat treated at 400 °C for 24 h.

porosity, grain boundaries, and triple junctions in the microstructure of nanocrystalline Ni. In this study, three nanocrystalline Ni layers with average grain size <100 nm were prepared by pulse plating and are shown in Fig. 10. The deviation in Hall–Petch behavior was also found, and the turning point is about 200 nm. The difference of the critical grain size can be due to different plating and thermal treatment. Various microstructures and defects (e.g., microflaws or porosities) are identified in the nanocrystalline Ni layers. For instance, a lot of

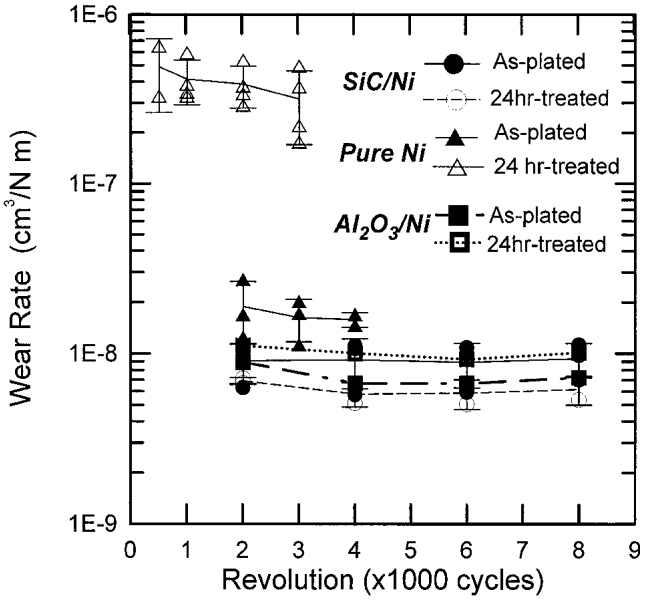

FIG. 7. Wear rate of the pure Ni, ultrafine SiC/Ni, and Al_2O_3/Ni composite layers as-plated or after heat treated at 400 °C for 24 h in N_2 atmosphere.

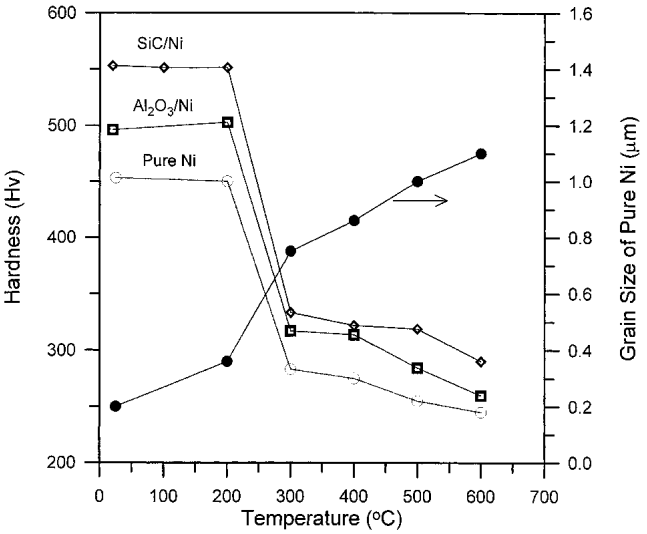

FIG. 8. Hardness of the pure Ni and ultrafine SiC/Ni and Al_2O_3/Ni composite layers and grain size of pure Ni changed with various heat-treated temperatures for 1 h.

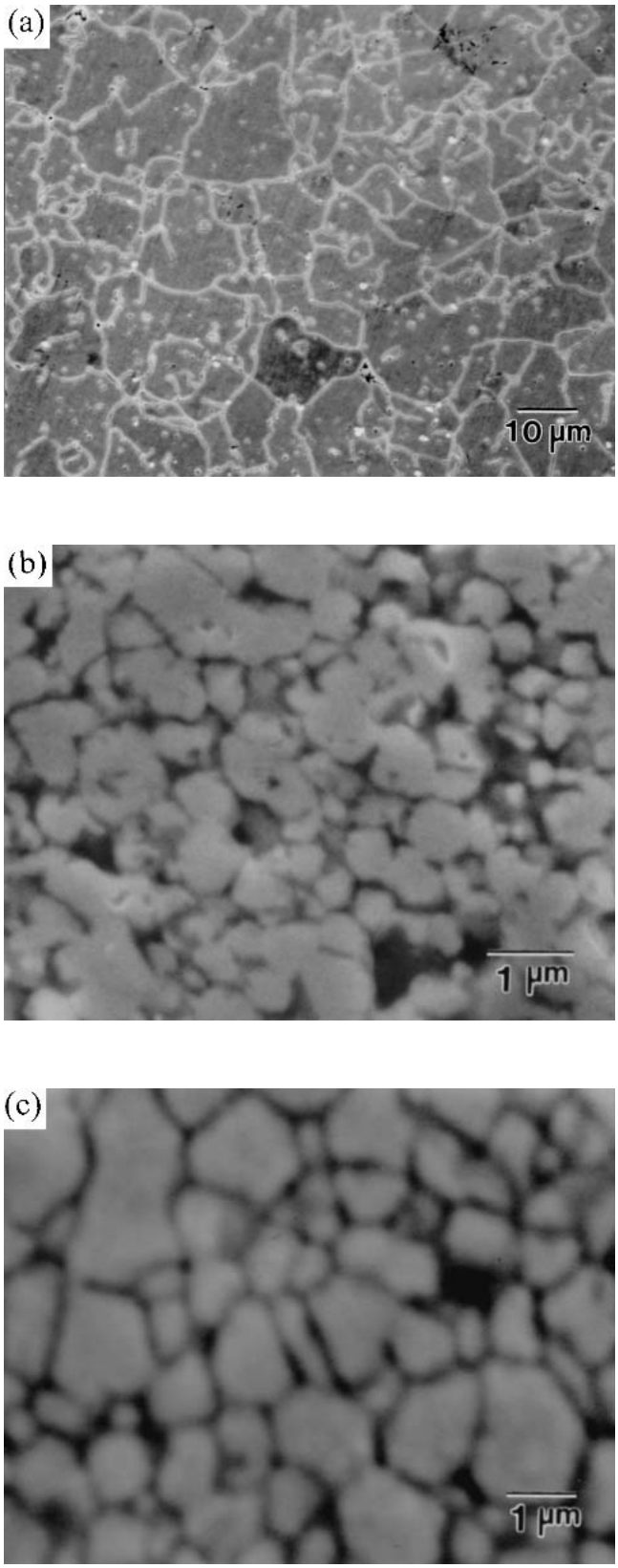

FIG. 9. SEM micrographs of acid-etched surfaces of the cross-sections of (a) pure Ni and ultrafine (b) SiC/Ni and (c) Al_2O_3/Ni composite layers. These specimens were heat treated at 400 °C for 24 h.

twins are found on TEM observation of the Ni grains. Therefore, two Hall–Petch equations can be fitted for each region either greater or smaller than 200 nm in Fig. 10. The first H-P equation ranges from 200 nm to 14 μm as below:

$$H_1 = 155\ d^{-0.5} + 101 \quad . \tag{2}$$

For the SiC/Ni (solid square) and Al_2O_3/Ni (solid circle) composites treated in the same conditions, the average hardness is slightly larger than the prediction of Eq. (2). For instance, the hardness of SiC/Ni composite is only 20 Hv larger than that (260 Hv) of the pure Ni in a grain size of 1.0 μm. This implies that, when the grain size of Ni is larger than 0.2 μm, the hardening mechanism of the pure Ni or Al_2O_3/Ni composite is well described by a Hall–Petch effect. The second mechanism (dispersive hardening effect) plays a minor effect and is only 20 Hv

TABLE I. The average grain size, shape, hardness, and wear rate of Ni grains in ultrafine SiC/Ni, and Al_2O_3/Ni composite layers and in pure Ni before and after 400 °C heat treatment for 24 h.

	As-deposited	Heat treated at 400 °C
Grain size of Ni (μm)		
pure Ni	0.20 × 2.0 (columnar grain)	14 (equiaxed grain)
SiC/Ni	0.078 (equiaxed grain)	1.0 (equiaxial)
Al_2O_3/Ni	0.089 (equiaxed grain)	1.4 (equiaxial)
Hardness (Hv)		
pure Ni	453	146
SiC/Ni	550	300
Al_2O_3/Ni	496	240
Wear rate (cm^3/N m)		
pure Ni	2×10^{-8}	4×10^{-7}
SiC/Ni	9×10^{-9}	7×10^{-9}
Al_2O_3/Ni	7×10^{-9}	1×10^{-8}

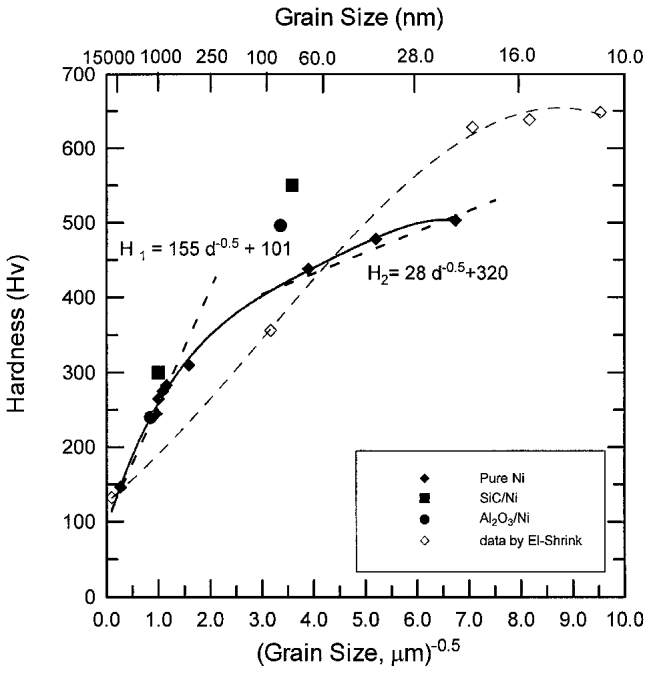

FIG. 10. Plot of hardness versus square root of the grain size of pure Ni, also included the hardness of the composite layers with either ultrafine SiC or Al_2O_3.

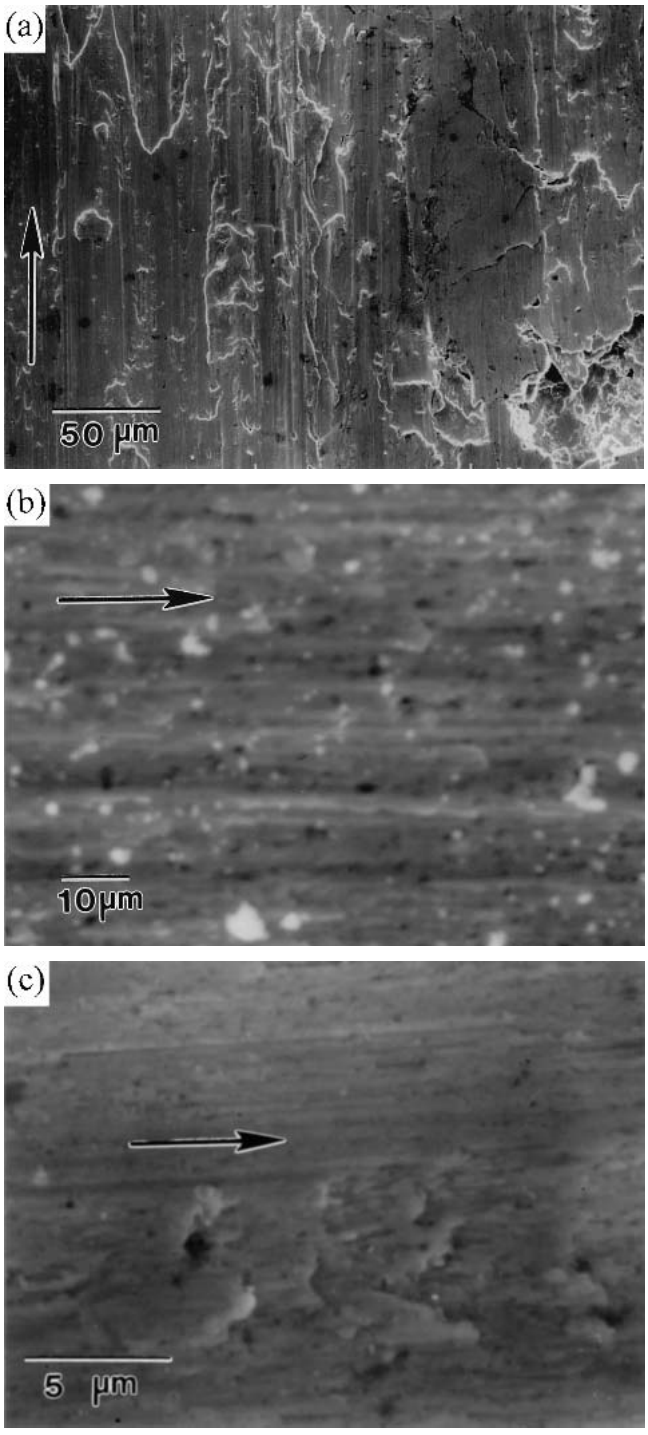

FIG. 11. SEM micrographs of the worn surfaces of (a) pure Ni and ultrafine (b) SiC/Ni and (c) Al_2O_3/Ni composite layers. The arrows indicate the wearing direction.

higher than pure Ni in the same matrix grain size. However, as the Ni grain size is smaller than 200 nm, the other H-P equation can be fitted as below:

$$H_2 = 28\ d^{-0.5} + 320 \quad . \tag{3}$$

The k value 28 in Eq. (3) is smaller than 155 of Eq. (2). It implies that the "locking parameter" of dislocation pileup or the relative hardening contribution of the grain boundaries is reduced for the nano-sized Ni grains.[23] The average Ni grain sizes of the untreated SiC/Ni and Al_2O_3/Ni composites are 78 and 89 nm, respectively. The hardness of these two composite layers is greater than that predicted by Eq. (3). In the same matrix grain size, the SiC/Ni and Al_2O_3/Ni nanocomposites show 150 and 100 Hv, respectively, higher than the pure Ni. It is believed that the hardness increments of the SiC/Ni and Al_2O_3/Ni nanocomposites are not only contributed by H-P effect, but also by the dispersive hardening effect. The SiC particles seem to have a better effect than the Al_2O_3 particles based on the same volume fraction of second phase.

B. Sliding wear resistance

For SiC/Ni composite prepared by composite electrodeposition, the micrometer size of SiC inclusions has adverse effects on the relative wear intensity of the Ni matrix.[24,25] As the SiC is larger than 15 μm, the relative wear intensity of composite is smaller than unity. (Relative wear intensity is defined as the volume loss of composite relative to the pure Ni in wear test.) However, the relative wear intensity is larger than unity as the average size of the added SiC is 5 μm. A similar result was reported for SiC particle larger than 5 μm and SiC/Ni ratio larger than 15 vol%.[26] The authors explained it was due to pull-out of particles. Figure 11 shows the worn surfaces of the pure Ni, SiC/Ni, and Al_2O_3/Ni composites. The hard particles grind the surface. That makes the surface of sample with several grooves. Grain-pullout and many cracks are formed perpendicular to the wearing direction on the surface of pure Ni. The surfaces have obvious redeposited matter (debris) coming from sliding wheel. Fe debris found on the worn surfaces of the SiC/Ni and Al_2O_3/Ni may be due to the interaction of hard particles with the wheel. The hardness of the wheel is about 800 HV; thus, abrasive SiC or Al_2O_3 particles are hard enough to plough into the surface of the wheel. The wearing also results in Fe debris, as the brightest features shown in Figs. 11(b) and 11(c). The evidences support the wearing of these Ni layers by tempered steel wheel to be adhesive wear. Ni grains are removed from the surface partially because of the adhesive reaction during the contact wearing. Consequently, the surface leaves various cavities.

According to the literature about adhesive wear, the wear rate can be described as a function of the work of adhesion (γ_{ad}), the standard deviation of asperity heights (S) of the worn surface, and inversely to the hardness (H) of specimen.[27–29]

$$\text{wear rate} = \frac{V}{F_N D} = \frac{\mathrm{K}}{H - \dfrac{\gamma_{ad}}{S}} \quad , \tag{4}$$

where V is the volume loss by the wear test, F_N is the normal stress, D is the distance of sliding, H is hardness (kg/mm^3), and K is a constant. The adhesive energy of Ni with the counter wheel (steel) decreases linearly by the addition of inert ceramic particles in the Ni layer.[24] Besides, the R_a of the ultrafine SiC/Ni, ultrafine Al_2O_3/Ni, and pure Ni are 0.93, 0.05, and 0.02 μm, respectively. The hardness and the standard deviation of asperity heights increase as the fraction of ultrafine ceramic particle increases. Consequently, all three factors, H, γ_{ad}, and S, favor the reduction of the wear rate when more SiC or Al_2O_3 particles are incorporated into the Ni matrix.

V. CONCLUSIONS

In this study, 7 vol% ultrafine SiC or Al_2O_3 particles were codeposited with Ni and randomly distributed in Ni matrix. The columnar Ni grains in pure Ni layer with the dimensions of 0.2 × 2 μm change to equiaxial shape of 78 and 89 nm for SiC/Ni and Al_2O_3/Ni composites, respectively. The preferred planes of the Ni grains change accordingly from (220) to (111) in the nanocomposite layers. Tiny Ni grains are formed in the regions between nanoceramic particles, which show the dimensions much smaller than the mean grain size. The addition of the ceramic particles provides the formation of tiny Ni grains during the stage of electroplating and inhibits the grain growth of Ni in thermal treatment.

The microhardness of the composite Ni layer increases about 20% as the ultrafine SiC particles added in Ni matrix increases. The hardening effects of the composites can be concluded as the grain refinement and secondary dispersive hardening. The hardness of Ni matrix begins to reduce at 300 °C for 1 h treatment; significant grain growth is found at that temperature. When the Ni grain-size ranges between a few micrometers to 200 nm, the hardening mechanism of the composites is dominated by Ni grain refinement. When the Ni grain size is smaller than 200 nm, the hardening effect is attributed both from grain refinement and dispersive hardening effects.

The friction coefficient of ultrafine SiC/Ni and Al_2O_3/Ni composite layers is slightly higher than that of pure Ni. However, the wear resistance of SiC/Ni and Al_2O_3/Ni composite coatings is significantly better than

that of pure Ni coating after the heat treatment at 400 °C for 24 h. The wear of the layers appears as a type of adhesive wear. The ultrafine ceramic particles significantly inhibit the grain growth of Ni grains above 300 °C, reduce adhesive work, and increase the deviation of asperity heights. SiC particles show a better retardant ability than ultrafine Al_2O_3 particles to the Ni matrix.

ACKNOWLEDGMENTS

The authors gratefully thank the National Science Council (NSC89-2216-E-002-016) for financial support, and also thank the engineers in the R & D Division, China Steel Company, for their assistance on electroplating.

REFERENCES

1. S.H. Yen and C.C. Wan, Mater. Sci. Technol. **11,** 589 (1995).
2. N. Guglielmi, J. Electrochem. Soc. **119,** 1009 (1972).
3. I. Shan, P.M. Vereecken, C.L. Chien, P.C. Searson, and R.C. Cammarata, J. Mater. Res. **17,** 1412 (2002).
4. A. Möller and H. Hahn, NanoStruct. Mater. **12,** 259 (1999).
5. H. Ferkel, B. Muller, and W. Riehemann, Mater. Sci. Eng. A **234–239,** 474 (1997).
6. R.R. Oberle, M.R. Scanlon, R.C. Cammarata, and P.C. Searson, Appl. Phys. Lett. **66,** 19 (1995).
7. M. Pushpavanam, Metal Finishing **95,** 22 (1997).
8. M. Viswanathan and M. Ghouse, Metal Finishing **77,** 67 (1979).
9. M. Ghouse, M. Viswanathan, and E.G. Ramachandran, Metal Finishing **78,** 31 (1980).
10. J. Zahavi and J. Hazan, Plating Surf. Finish. **69,** 57 (1982).
11. M. Ghouse, Metal Finish. **82,** 33 (1984).
12. N. Perienė, A. Češunienė, and L. Taicas, Plating Surf. Finish. **80,** 73 (1993).
13. K.N. Sun, X.N. Hu, J.H. Zhang, and J.R. Wang, Wear **196,** 295 (1996).
14. V.D. Stankovic and M. Gojo, Surf. Coat. Technol. **81,** 225 (1996).
15. R.N. Katz, Science **208,** 841 (1980).
16. R.C. Phoenix and W.D. Long, in *Ceramics for High Performance Applications III*, edited by E.M. Lenoe, R.N. Katz and J.J. Burke (Plenum Press, New York, 1983), pp. 395–400.
17. E. Orowan, in *Symposium on Internal Stresses* (Institute of Metals, London, U.K., 1947), p. 451.
18. K.H. Zum Gahr, Metal Prog. **116,** 46 (1979).
19. JCPDS File No. No.4-850 (International Center for Diffraction Data, Newton Square, PA, 1953).
20. S.C. Wang and W.J. Wei, Mater. Chem. Phy. **78,** 574 (2002).
21. M. Furukawa, Z. Horita, M. Nemoto, R.Z. Valiev, and T.G. Langdon, Acta Mater. **44,** 4619 (1996).
22. A.M. El-Sherik, U. Erb, G. Palumbo, and K.T. Aust, Scr. Metall. Mater. **27,** 1185 (1992).
23. G.E. Dieter, *Mechanical Metallurgy*, SI Metric ed. (McGraw-Hill, London, U.K., 1988), Chap. 6, pp.184–240.
24. K.H. Zum Gahr, in *Microstructure and Wear of Materials*, Tribol. Ser. 10 (Elsevier, Amsterdam, The Netherlands, 1987), Chap. 6, pp. 351–477.
25. K-H. Zum Gahr, Tribol. Int. **31,** 587 (1998).
26. I. Garcia, J. Fransaer, and J.P. Celis, Surf. Coat. Technol. **148,** 171 (2001).
27. J.T. Burwell and C.D. Strang, J. Appl. Phys. **23,** 18 (1952).
28. J.F. Archard, in *Wear Control Handbook,* edited by M.B. Peterson and W.O. Winer (ASME, New York, 1980), pp. 35–80.
29. H.M. Pollock and S.K. Roy Chowdhury, in *Microscopic Aspects of Adhesion and Lubrication. Tribol.* Ser. 7, edited by J.M. Georges (Elsevier, Amsterdam, The Netherlands, 1982), pp. 253–261.